RESEARCH ARTICLE

Intercellular Diffusion of a Fluorescent Sucrose Analog via the Septal Junctions in a Filamentous Cyanobacterium

Dennis J. Nürnberg,[a] Vicente Mariscal,[b] Jan Bornikoel,[c] Mercedes Nieves-Morión,[b] Norbert Krauß,[a] Antonia Herrero,[b] Iris Maldener,[c] Enrique Flores,[b] Conrad W. Mullineaux[a]

School of Biological and Chemical Sciences, Queen Mary University of London, London, United Kingdom[a]; Instituto de Bioquímica Vegetal y Fotosíntesis, Consejo Superior de Investigaciones Científicas and Universidad de Sevilla, Seville, Spain[b]; Department of Microbiology/Organismic Interactions, University of Tübingen, Tübingen, Germany[c]

D.J.N. and V.M. contributed equally to this work.

ABSTRACT **Many filamentous cyanobacteria produce specialized nitrogen-fixing cells called heterocysts, which are located at semiregular intervals along the filament with about 10 to 20 photosynthetic vegetative cells in between. Nitrogen fixation in these complex multicellular bacteria depends on metabolite exchange between the two cell types, with the heterocysts supplying combined-nitrogen compounds but dependent on the vegetative cells for photosynthetically produced carbon compounds. Here, we used a fluorescent tracer to probe intercellular metabolite exchange in the filamentous heterocyst-forming cyanobacterium *Anabaena* sp. strain PCC 7120. We show that esculin, a fluorescent sucrose analog, is incorporated by a sucrose import system into the cytoplasm of *Anabaena* cells. The cytoplasmic esculin is rapidly and reversibly exchanged across vegetative-vegetative and vegetative-heterocyst cell junctions. Our measurements reveal the kinetics of esculin exchange and also show that intercellular metabolic communication is lost in a significant fraction of older heterocysts. SepJ, FraC, and FraD are proteins located at the intercellular septa and are suggested to form structures analogous to gap junctions. We show that a Δ*sepJ* Δ*fraC* Δ*fraD* triple mutant shows an altered septum structure with thinner septa but a denser peptidoglycan layer. Intercellular diffusion of esculin and fluorescein derivatives is impaired in this mutant, which also shows a greatly reduced frequency of nanopores in the intercellular septal cross walls. These findings suggest that FraC, FraD, and SepJ are important for the formation of junctional structures that constitute the major pathway for feeding heterocysts with sucrose.**

IMPORTANCE ***Anabaena*** **and its relatives are filamentous cyanobacteria that exhibit a sophisticated form of prokaryotic multicellularity, with the formation of differentiated cell types, including normal photosynthetic cells and specialized nitrogen-fixing cells called heterocysts. The question of how heterocysts communicate and exchange metabolites with other cells in the filament is key to understanding this form of bacterial multicellularity. Here we provide the first information on the intercellular exchange of a physiologically important molecule, sucrose. We show that a fluorescent sucrose analog can be imported into the *Anabaena* cytoplasm by a sucrose import system. Once in the cytoplasm, it is rapidly and reversibly exchanged among all of the cells in the filament by diffusion across the septal junctions. Photosynthetically produced sucrose likely follows the same route from cytoplasm to cytoplasm. We identify some of the septal proteins involved in sucrose exchange, and our results indicate that these proteins form structures functionally analogous to metazoan gap junctions.**

Received 7 October 2014 **Accepted** 11 February 2015 **Published** 17 March 2015

Citation Nürnberg DJ, Mariscal V, Bornikoel J, Nieves-Morión M, Krauß N, Herrero A, Maldener I, Flores E, Mullineaux CW. 2015. Intercellular diffusion of a fluorescent sucrose analog via the septal junctions in a filamentous cyanobacterium. mBio 6(2):e02109-14. doi:10.1128/mBio.02109-14.

Invited Editor Elisabeth Gantt, University of Maryland, College Park **Editor** Douglas G. Capone, University of Southern California

Address correspondence to Conrad W. Mullineaux, c.mullineaux@qmul.ac.uk, Enrique Flores, eflores@ibvf.csic.es, or Iris Maldener, iris.maldener@mikrobio.uni-tuebingen.de.

The filamentous cyanobacterium *Anabaena* sp. strain PCC 7120 (here *Anabaena*) is a multicellular prokaryote. Simultaneous oxygenic photosynthesis and nitrogen fixation are achieved by locating the oxygen-sensitive nitrogenase in specialized differentiated cells called heterocysts. Heterocyst differentiation involves complex metabolic and morphological changes (1, 2). During combined-nitrogen starvation, heterocysts form at intervals of 10 to 20 cells, establishing a spacing pattern along the filament (3) that may be controlled by a diffusible product of the *patS* gene acting on the master regulator HetR (4–6). Heterocysts maintain a microoxic cytoplasm by building extra envelope layers as diffusion barriers to O_2 (7) and by dismantling photosystem II and activating respiration (1, 2). Heterocysts and vegetative cells are mutually dependent: while vegetative cells supply carbon skeletons, heterocysts supply combined-nitrogen compounds (1, 2). Likely vehicles for combined-nitrogen supply from heterocysts to vegetative cells are glutamine (8, 9) and β-aspartyl-arginine, a breakdown product of the storage compound cyanophycin (10, 11). The most likely carrier of fixed carbon is sucrose, since diazotrophic growth requires sucrose production in the vegetative

cells and breakdown by invertases in the heterocysts (12–15). However, amino acids such as glutamate and alanine may also be transferred to heterocysts (16, 17).

In *Anabaena*, two routes of intercellular metabolite exchange have been proposed (18–20): either via a continuous periplasm (21, 22) or by diffusion from cytoplasm to cytoplasm via cell-cell connections (23) involving the septal proteins SepJ (also known as FraG) (24, 25), FraC, and FraD (26, 27). These proteins are likely components of structures that have been termed microplasmodesmata (28, 29) or septosomes (30). Analyses of deletion mutants show the importance of these proteins for filament integrity, diazotrophic growth, and intercellular communication, consistent with the idea that SepJ, FraC, and FraD form structures that allow the intercellular movement of small cytoplasmic molecules (23–27). By analogy with metazoan gap junctions (reviewed in reference 31), these structures have been termed septal junctions (32).

The murein sacculus is generally thicker in cyanobacteria than in the most widely studied Gram-negative bacteria, such as *Escherichia coli*, but thinner than in Gram-positive bacteria (33–35). Thus, the cyanobacterial murein sacculus is likely composed of several peptidoglycan layers. In *Anabaena*, the thickness of the murein sacculus may correspond to two interlinked peptidoglycan layers (30). Murein sacculi have been isolated from several heterocyst-forming cyanobacteria, and sacculi corresponding to several cell units have been obtained (36–38). This implies that the peptidoglycan layers of adjacent cells are fused in a substantial fraction of the intercellular septa of a filament. In material isolated from *Nostoc punctiforme*, the septal peptidoglycan can be seen by electron microscopy as discs containing holes about 20 nm in diameter that have been termed nanopores and are relevant for intercellular communication (38). Nanopores in the intercellular peptidoglycan would be required to accommodate protein structures linking the cytoplasms of adjacent cells. The low-density areas observed by electron microscopy in the intercellular peptidoglycan of *Anabaena* (30), *Anabaena variabilis* (39), and *Mastigocladus laminosus* (40) likely correspond to the septal peptidoglycan nanopores. Additionally, an electron tomographic study of the septum between cells in *Anabaena* shows that these structures are also present between vegetative cells and heterocysts (41). Cell wall amidases AmiC2 (NpF1846) and AmiC1 (Alr0092), which have been recently characterized in *N. punctiforme* and *Anabaena*, respectively (37, 42), are required to make the septal peptidoglycan nanopores. Mutants lacking these proteins are impaired in cell differentiation and exchange of the fluorescent tracer molecule calcein, suggesting that modification of the septal peptidoglycan by these enzymes is essential for intercellular communication (38, 43).

Intercellular communication in filamentous cyanobacteria has been studied by using fluorescence recovery after photobleaching (FRAP). FRAP requires a suitable fluorescent tracer to be introduced into the appropriate cell compartment. Periplasmic communication was studied by expressing green fluorescent protein (GFP) (22, 44) or the smaller fluorescent protein iLOV (45) exported into the periplasm via the twin-arginine translocation system. GFP is not exchanged from cytoplasm to cytoplasm, but cytoplasmic exchange could be examined by loading the smaller fluorescent tracer molecules calcein and 5-carboxyfluorescein (5-CF) into the cytoplasm of *Anabaena* (23, 46) and other filamentous cyanobacteria (23, 38, 40) by using an esterified cell-permeating precursor that is processed by cytoplasmic esterases to release a hydrophilic fluorescent product. FRAP reveals rapid transfer of calcein and 5-CF between the cytoplasms of adjacent cells, impaired in mutants lacking SepJ, FraC, or FraD (23, 26, 46).

Plant sucrose uptake transporters (SUTs) (47) have been studied by monitoring the uptake of the fluorescent coumarin β-glucoside esculin (48, 49). Type I SUTs import esculin at a rate similar to that of sucrose (47, 50), showing that esculin is recognized and transported similarly to sucrose. Here we explore the uptake and intercellular exchange of esculin in *Anabaena*. Fluorescence microscopy and FRAP show that esculin is imported into the cytoplasm and can then be exchanged rapidly and reversibly among vegetative cells and between vegetative cells and heterocysts. A triple mutant lacking SepJ, FraC, and FraD is impaired in intercellular esculin exchange. Compared to the wild type, it shows an altered peptidoglycan structure and a much lower frequency of nanopores in the peptidoglycan at the intercellular cross walls.

RESULTS

An *Anabaena* Δ*sepJ* Δ*fraC* Δ*fraD* triple mutant shows an altered peptidoglycan structure and fewer nanopores in the septal cross walls. *Anabaena* Δ*sepJ* and Δ*fraC* Δ*fraD* mutants have been previously constructed (26, 27, 46). To test whether the simultaneous inactivation of *fraC*, *fraD*, and *sepJ* has any additional effect compared to the inactivation of *fraC* and *fraD* or of *sepJ*, a triple mutant was created by transfer of a *sepJ*-inactivating construct to Δ*fraC* Δ*fraD* mutant strain CSVT22 (27). Strain CSVM141 has the predicted deletions in the three genes and lacks wild-type copies of these genes (see Fig. S1 in the supplemental material). Similarly to strains CSVT22 (Δ*fraC* Δ*fraD*) and CSVM34 (Δ*sepJ*), strain CSVM141 grew well in medium with combined nitrogen (nitrate or ammonium). In the presence of nitrate and culture treatment in accordance with the protocol described in Materials and Methods, CSVM141 formed filaments generally shorter than those of the wild type but longer than those found in the Δ*sepJ* and Δ*fraC* Δ*fraD* mutants (see Fig. S2 in the supplemental material). Transfer to $BG11_0$ medium, which lacks combined-nitrogen compounds, led to rapid fragmentation of CSVM141 filaments (see Fig. S2B), resulting in very short filaments after 48 h (see Fig. S2C). CSVM141 therefore cannot form heterocysts or grow diazotrophically.

To assess whether the absence of the three septal proteins could influence septal characteristics, we studied the intercellular septa in CSVM141 and wild-type filaments grown with combined nitrogen. Transmission electron microscopy (TEM) showed that the cell junctions in the triple mutant were significantly thinner than in the wild type (Fig. 1A). The distance (mean ± standard deviation [SD]; *n*, number of junctions measured) between the cytoplasmic membranes of adjacent cells was 27.7 ± 1.12 nm ($n = 16$) for CSVM141 and 37.3 ± 1.93 ($n = 23$) for the wild type (Student's *t* test, $P = 3.3 \times 10^{-23}$). In CSVM141, a particularly electron-dense layer could be detected between the adjacent cells, indicative of an increased density of septal peptidoglycan.

To study peptidoglycan in more detail, labeling with fluorescent vancomycin (Van-FL), which marks peptidoglycan that is in the process of growth or remodeling (38), was performed. Van-FL strongly labeled the intercellular septa in the wild type and the Δ*fraC* Δ*fraD* mutant but much less strongly in the Δ*sepJ* and triple mutants (Fig. 1B). In the wild type and the Δ*fraC* Δ*fraD* mutant, there was a broad spread in the level of Van-FL labeling (see Fig. S3

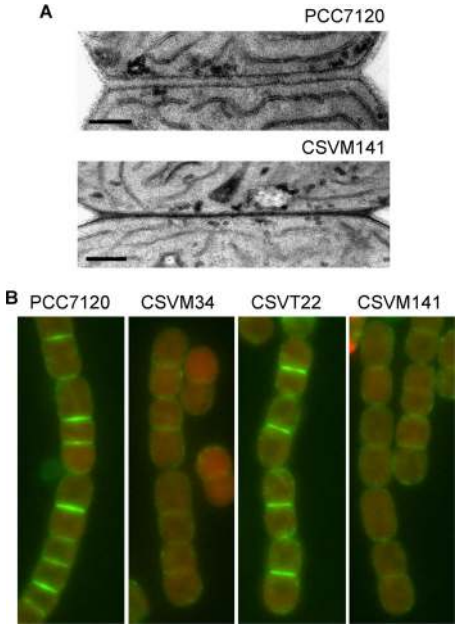

FIG 1 Ultrastructure and remodeling of the septal peptidoglycan in wild-type *Anabaena* and mutant strains lacking septal proteins. (A) Transmission electron micrographs of the septum between two vegetative cells of wild-type *Anabaena* (top) and between two vegetative cells of strain CSVM141 (Δ*sepJ* Δ*fraC* Δ*fraD*) (bottom). Scale bars, 200 nm. (B) Fluorescence micrographs showing labeling with Van-FL in wild-type *Anabaena* and mutants CSVM34 (Δ*sepJ*), CSVT22 (Δ*fraC* Δ*fraD*), and CSVM141 (Δ*sepJ* Δ*fraC* Δ*fraD*).

in the supplemental material). The Δ*sepJ* mutant and especially CSVM141 showed very few highly labeled septa, implying lower peptidoglycan turnover or remodeling rates in the intercellular septa in the absence of SepJ.

We then investigated whether the arrays of septal peptidoglycan nanopores that have been identified in *N. punctiforme* (38) and *Anabaena* (43) are still present in the mutants lacking the septal proteins. Isolated sacculi were visualized by TEM, and a total of 5 to 10 septa of each mutant were inspected (examples shown in Fig. 2; see Fig. S4 in the supplemental material). The mean number of nanopores was considerably lower in the three mutants than in the wild type (Fig. 2, histogram). Interestingly, the septal peptidoglycan nanopores had significantly greater diameter in the three mutants than in the wild type, and this was particularly evident in the strains lacking FraC and FraD (see Fig. S5 in the supplemental material). Thus, the septal proteins (SepJ, FraC, and FraD) are involved in septal peptidoglycan nanopore formation, but it should be noted that some residual nanopores are still retained even in the triple mutant (Fig. 2).

The *Anabaena* Δ*sepJ* Δ*fraC* Δ*fraD* triple mutant is impaired in intercellular molecular exchange of tracer dyes. The fluorescein derivatives calcein and 5-CF (Table 1) can be loaded into the *Anabaena* cytoplasm and used to measure the kinetics of intercellular molecular exchange in confocal FRAP measurements (23, 27). These artificial dyes move from cytoplasm to cytoplasm via the septal junctions, and any involvement of the periplasm is unlikely (23). The Δ*sepJ* mutant shows a decreased rate of calcein exchange (23, 27, 46), and Δ*fraC* and Δ*fraD* mutants and the Δ*fraC* Δ*fraD* double mutant show decreased rates of exchange of both 5-CF and calcein (27). However, these mutants show a residual exchange activity of about 20% of the wild-type activity. To determine whether this residual exchange is affected by a combination of these mutations, we studied the intercellular exchange of calcein and 5-CF in the triple mutant by using the rate constant for fluorescence recovery of the bleached cell (*R*) as a simple measure of molecular exchange activity (27). Rates of calcein exchange between vegetative cells of the triple mutant were similar to those observed in the Δ*sepJ* and Δ*fraC* Δ*fraD* mutants, and 5-CF exchange rates were similar to those of the Δ*fraC* Δ*fraD* double mutant (Table 2). These results imply the existence of an additional pathway or mechanism, independent of the known septal proteins, for the intercellular exchange of calcein and 5-CF that contributes about 20% of the wild-type activity. An obvious possibility is that there are additional, as yet uncharacterized, channel-forming proteins responsible for this residual exchange activity and associated with the small number of remaining septal nanopores in the triple mutant (Fig. 2).

Uptake of esculin by *Anabaena*. Calcein and 5-CF are fluorescein derivatives with no resemblance to any metabolites known to be physiologically important in *Anabaena*. Therefore, to provide more physiologically relevant information on intercellular molecular exchange, we set out to find a usable fluorescent analog of sucrose, which appears to be a key vehicle for fixed carbon transfer from vegetative cells to heterocysts (12–15). We reasoned that such a molecule might be actively imported into the cytoplasm by native sucrose uptake systems, thus removing the need to use cell-permeant ester derivatives as with calcein and 5-CF (23, 27). Several fluorescent sucrose analogs have been used to monitor sucrose uptake in plants, including rutin, quercetin, and esculin (50). We found that esculin was significantly incorporated and retained in *Anabaena* cells (Fig. 3). Comparison of the distributions of esculin and chlorophyll fluorescence from the thylakoid membranes shows that esculin fluorescence originates from the cytoplasm (Fig. 3A). Esculin fluorescence could not be detected in the periplasm, where fluorophores make a fluorescent halo outside the thylakoid membranes (22, 44, 45). Figure S6 compares the distributions of esculin fluorescence with chlorophyll and periplasmic GFP. Since the periplasm is a thin compartment, we cannot exclude the presence of some esculin in the periplasm, but it is clear that at least most of the esculin must be in the cytoplasm. Similarly to calcein (23), esculin fluorescence is somewhat depleted in the thylakoid membrane region (Fig. 3A; see Fig. S6 in the supplemental material), confirming that esculin is located in the cytoplasm rather than in the thylakoid lumen. Nearly all filaments show esculin fluorescence, but significant variation in fluorescence intensity (Fig. 3A) indicates variation in esculin uptake competence.

Esculin fluorescence is pH dependent (51), and fluorescence emission spectra at pH 4.5 to 10 show that the fluorescence yield increases with the pH (see Fig. S7A in the supplemental material). The cytoplasmic pH of *Anabaena* vegetative cells is about 7.0 when they are grown in BG11 medium (52). Assuming that the pH in other cell compartments falls within the range of 6.5 to 8.0, esculin fluorescence yield would be similar to within a factor of ~0.8 to 1.3 (see Fig. S7A). We found that esculin fluorescence is unaffected by O_2 concentration (see Fig. S7B), and therefore, comparison of fluorescence in vegetative cells and heterocysts should not be problematic.

Anabaena expresses sucrose transport activity (53). To test whether esculin is taken up by a specific sucrose transporter, we

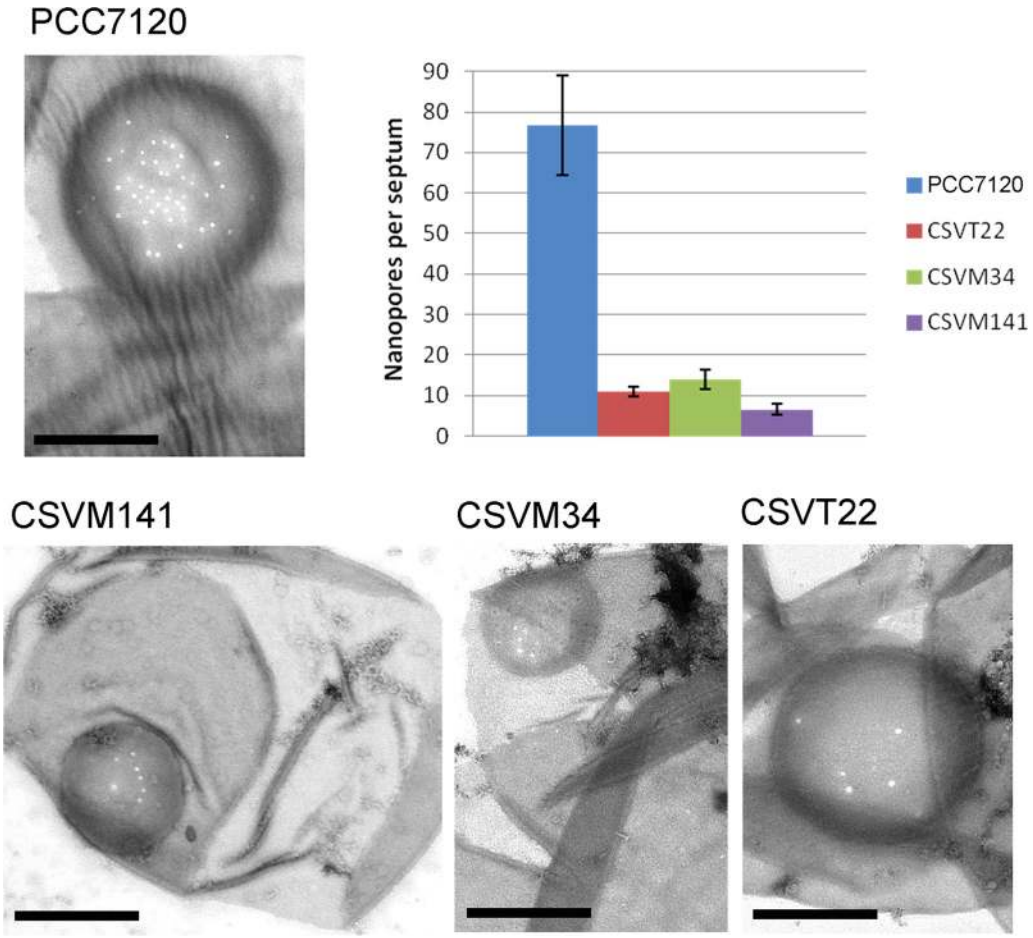

FIG 2 Septal nanopores in *Anabaena*. Shown are representative transmission electron micrographs of sacculi from wild-type *Anabaena* and mutants CSVM34 (Δ*sepJ*), CSVT22 (Δ*fraC* Δ*fraD*), and CSVM141 (Δ*sepJ* Δ*fraC* Δ*fraD*) (scale bars, 500 nm). For further examples, see Fig. S4 in the supplemental material. The histogram shows the mean number of nanopores per septum ± SD for the different strains. Student's *t* tests showed that the differences between the wild type and all of the mutants were significant (CSVT22, $P = 5.9 \times 10^{-3}$; CSVM34, $P = 7 \times 10^{-3}$; CSVM141, $P = 3.7 \times 10^{-3}$).

developed a fluorometric assay for esculin uptake (Fig. 4). Esculin was taken up linearly for at least 70 min. Addition of sucrose greatly reduced the rate of esculin uptake, suggesting that both molecules compete for the same uptake mechanism (Fig. 4).

Esculin as a fluorescent probe for intercellular communication. FRAP experiments to probe intercellular communication use a confocal laser scanning microscope to bleach fluorescence in one or more cells. The subsequent redistribution of fluorescence between cells reveals the kinetics of intercellular exchange of the fluorophore (23). Experiments with esculin were less straightforward than those with fluorescein derivatives. There is weak but detectable background autofluorescence from the cells at the wavelengths used for esculin detection (Fig. 3B), and esculin fluorescence is easily bleached while recording image series in the confocal microscope. By using low laser power and a wide confocal pinhole for efficient light collection at the expense of resolution

TABLE 1 Predicted physicochemical properties of esculin, sucrose, and the hydrolyzed intracellular forms of two fluorescein derivatives used to probe intercellular communication in *Anabaena*[a]

Parameter	Sucrose	Esculin	Calcein	5-CF
Molecular mass (Da)	342.3	340.3	622.5	376.3
Polar surface area (Å^2)	189.5	145.9	231.7	113.3
Solvent-accessible molecular surface area (Å^2)	456.5	414.6	794.8	448.4
Van der Waals volume (Å^3)	289.0	278.0	510.4	299.1
Minimal projection area (Å^2)	57.1	45.8	67.0	59.2
Length perpendicular to minimal projection area(Å)	11.5	14.8	19.7	13.1
Maximal projection area (Å^2)	78.0	90.1	139.1	91.0
Length perpendicular to maximal projection area (Å)	9.2	7.0	10.4	9.7
Charge(s) of different species at pH 7.0 (% abundance[s])	0 (100)	0 (93), −1 (7)	−3 (48), −2 (25), −4 (25), −5 (2)	−1 (98), −2 (2)

[a] See references 23, 26, 27, and 46. Properties are predicted for pH 7.0, corresponding to the pH in the cytoplasm of vegetative cells (52).

TABLE 2 Rates of calcein and 5-CF exchange between wild-type and mutant vegetative *Anabaena* cells[a]

Anabaena strain	Mean R (s^{-1}) ± SD (n)	
	Calcein	5-CF
PCC 7120 (wild type)	0.097 ± 0.023 (18)	0.080 ± 0.013 (37)
CSVM34 (Δ*sepJ*)	0.023 ± 0.007 (12)	0.054 ± 0.007 (54)
CSVT22 (Δ*fraC* Δ*fraD*)	0.015 ± 0.003 (21)	0.017 ± 0.003 (42)
CSVM141 (Δ*sepJ* Δ*fraC* Δ*fraD*)	0.028 ± 0.006 (21)	0.022 ± 0.002 (84)

[a] Calcein and 5-CF were loaded into cells of BG11-grown filaments of the strains indicated, the tracer was bleached in one cell, and the fluorescence recovery rate constant, R, was determined as described in Materials and Methods. Data are mean values ± SDs (12 to 84 filaments were analyzed for each strain and tracer). Student's t tests indicate that differences in calcein transfer between strains PCC 7120 and CSVM34 and between PCC 7120 and CSVT22 are significant ($P < 10^{-4}$) and the difference between CSVM141 and CSVT22 might also be significant ($P = 0.04$). Differences in 5-CF transfer between strains PCC7120 and CSVM34, PCC7120 and CSVT22, CSVM34 and CSVT22, and CSVM141 and CSVT34 are all significant ($P < 10^{-5}$).

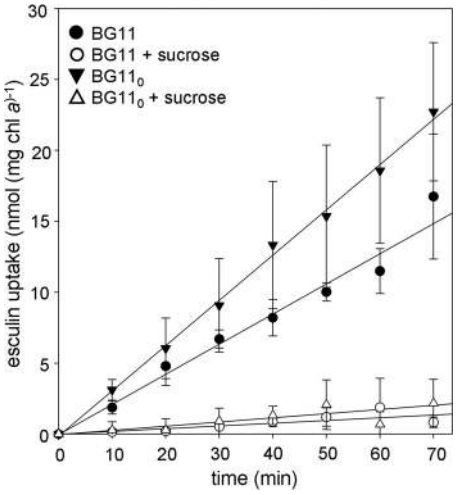

FIG 4 Time course of esculin uptake in *Anabaena* cells and effect of sucrose competition. Cells were grown in BG11 or BG11$_0$ medium with or without combined nitrogen. Uptake of esculin (100 μM) was measured with or without sucrose at 10 mM. Error bars represent SDs ($n = 3$ to 5). Rates of uptake differed significantly for BG11 with or without sucrose ($P = 0.00003$), BG11$_0$ with or without sucrose ($P = 0.002$), and BG11 versus BG11$_0$ without sucrose ($P = 0.05$). Absolute esculin uptake values assume that the intracellular fluorescence yield is similar to that in the buffer.

in the z direction, we could record repeat images with negligible photobleaching. An important control is to test for the possibility of spontaneous recovery from photobleaching by bleaching out the entire filament, so that there is no possibility of fluorescence recovery due to redistribution of the fluorophore. Such a control indicates a spontaneous recovery of about 7.5% of the initial fluorescence (Table 3), which complicates data analysis. Finally, esculin FRAP measurements always showed incomplete fluorescence recovery, similarly to 5-CF (27). This incomplete recovery indicates that a proportion of esculin cannot be exchanged between cells, accounting for ~50 to 75% of the esculin fluorescence (Table 3). Esculin binds to some proteins (54), and there could be specific sucrose-binding factors in the cytoplasm. Protein-bound esculin will probably be unavailable for intercellular exchange by any route. The septal junctions are impermeable to GFP and therefore must have a pore size that excludes many (and possibly all) proteins (4, 22). The immobile fraction precluded accurate quantitation of the "exchange coefficient" E (23) among vegetative cells. E relates the rate of dye movement between two adjacent cells to the difference in dye concentration between the cells, and its quantitation requires fitting of the simulated time development of dye distribution in the filament to the experimental data (23). Here, we used a simpler way to quantify kinetics of esculin transfer between vegetative cells by measuring the recovery rate constant R as previously described (27; see Materials and Methods).

Intercellular diffusion of esculin in *Anabaena* filaments. We used FRAP to probe the intercellular transfer of esculin in *Anabaena* filaments by bleaching esculin fluorescence in a single cell and monitoring its fluorescence recovery over time (Fig. 5). In differentiated filaments, we bleached esculin fluorescence in veg-

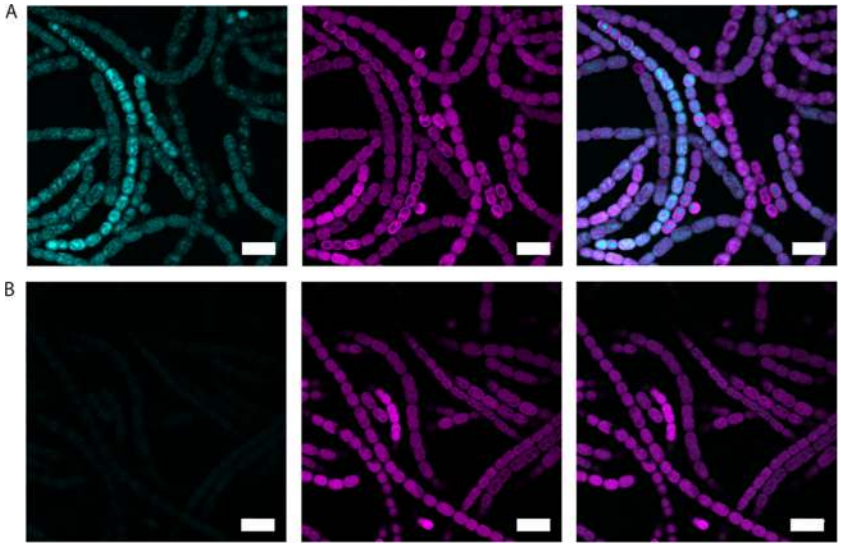

FIG 3 Uptake of esculin by wild-type *Anabaena* filaments. (A) Esculin-labeled cells (grown in BG11). (B) Control with unlabeled cells. Scale bars, 10 μm. Esculin fluorescence (443 to 490 nm) is cyan (left), chlorophyll fluorescence (670 to 720 nm) is magenta (center), and overlaid images are shown on the right.

TABLE 3 Kinetics of esculin exchange from FRAP measurements on *Anabaena* filaments[a]

Measurement (no. of replicates)	Mean R (s^{-1}) ± SD	Mean F_i ± SD
Vegetative cells in presence of nitrate		
Wild-type *Anabaena* (29)*	0.137 ± 0.050	0.518 ± 0.143
CSVM34 (Δ*sepJ*) (25)†	0.099 ± 0.042	0.571 ± 0.145
CSVT22 (Δ*fraC* Δ*fraD*) (30)‡	0.069 ± 0.029	0.605 ± 0.072
CSVM141 (Δ*sepJ* Δ*fraC* Δ*fraD*) (21)§	0.069 ± 0.030	0.671 ± 0.068
Vegetative cells of wild-type *Anabaena* 48 h after nitrogen deprivation (38)¶	0.142 ± 0.046	0.507 ± 0.110
Heterocysts 48 h after nitrogen deprivation		
Wild-type *Anabaena* (33)**	0.060 ± 0.054	0.757 ± 0.069
CSVT22 (Δ*fraC* Δ*fraD*) (18)††	0.017 ± 0.024	0.736 ± 0.097
CSS7 (*cphA1*::C.S3) (24)	0.074 ± 0.069	0.640 ± 0.160
Spontaneous fluorescence recovery of wild-type *Anabaena* (21)		0.925 ± 0.049

[a] The mean exponential recovery rate constants (R) and immobile fractions (F_i) for filaments grown with or without combined nitrogen were measured. R values were standardized by dividing by 2 for cells with two connecting junctions (i.e., all of the cells except those at the terminus of the filament). F_i is defined by $(I_I - I_E)/(I_I - I_0)$, where I_I is the initial fluorescence intensity before bleaching, I_0 is the fluorescence intensity immediately after bleaching, and I_E is the final fluorescence intensity. The extent of spontaneous fluorescence recovery is given by $1 - F_i$. Student's t tests show that R is significantly different between * and † ($P = 0.004$), * and ‡ ($P < 0.00001$), * and § ($P < 0.00001$), † and ‡ ($P = 0.004$), † and § ($P = 0.008$), ** and †† ($P = 0.002$), * and ** ($P < 0.00001$), ‡ and †† ($P < 0.00001$), and ¶ and ** ($P < 0.00001$). R values for cells showing $1 - F_i = <0.075$ (equivalent to the spontaneous fluorescence recovery in the absence of diffusion) were considered to be 0.

etative cells and in heterocysts, which could be distinguished by their enlarged size and reduced chlorophyll fluorescence. Both cell types show recovery under all of the conditions tested, indicating that esculin can be transferred between vegetative cells (Fig. 5A and B) and from vegetative cells to heterocysts (Fig. 5C and D). Fluorescence recovery greatly exceeds the spontaneous recovery of esculin fluorescence (Table 3), showing that there is intercellular molecular exchange. Esculin transfer shows the characteristics of diffusion rather than active transport, since fluorescent esculin always flows down the concentration gradient and the transfer runs to equilibrium (Fig. 5). Reversibility of esculin transfer from vegetative cells to heterocysts was tested by bleaching vegetative cells neighboring a heterocyst. If a single vegetative cell next to a heterocyst is bleached, fluorescence recovery mainly reflects molecular exchange with the next vegetative cell rather than with the heterocyst because of the faster exchange among vegetative cells (Table 3). Therefore, we chose a short filament of *Anabaena* with a terminal heterocyst and bleached esculin fluorescence in all of the vegetative cells. The subsequent decay of heterocyst fluorescence (Fig. 5E and F) shows that esculin can be transferred from heterocysts to vegetative cells. Esculin transfer occurs at comparable rates in both directions (Fig. 5D and F), indicating intercellular diffusion of esculin without significant active transport. Esculin fluorescence is not observed conspicuously or consistently at the periphery of the cells (Fig. 3A; see Fig. S6 in the supplemental material), suggesting that exchange occurs predominantly from cytoplasm to cytoplasm, resembling the previously characterized intercellular diffusion of calcein and 5-CF (23, 27).

Kinetics of esculin exchange and influence of septal proteins SepJ, FraC, and FraD. In wild-type *Anabaena* filaments, esculin exchange is significantly faster among vegetative cells than between vegetative cells and heterocysts (Table 3), although the difference is less pronounced than with calcein (23). Esculin exchange among vegetative cells did not become significantly faster following combined-nitrogen removal (Table 3), in contrast to calcein (23). Esculin influx into heterocysts is not significantly faster in a mutant that lacks the cyanophycin synthetase CphA1 and is therefore unable to form cyanophycin plugs at the heterocyst cell poles (55) (Table 3). This indicates that esculin transfer is not retarded by any cyanophycin plugs that may be present. Consistent with this finding, we could not detect any interaction between esculin and cyanophycin *in vitro* (see Fig. S8 in the supplemental material).

SepJ, FraC, and FraD are important for the intercellular exchange of fluorescent tracers (23, 27, 46). We investigated the influence of these proteins on the intercellular transfer of esculin by using Δ*sepJ*, Δ*fraC* Δ*fraD*, and Δ*sepJ* Δ*fraC* Δ*fraD* mutants as described above. These mutants show filament fragmentation under some conditions (24, 26) (see Fig. S2 in the supplemental material); however, we always chose filaments at least 5 cells long for FRAP measurements. In BG11-grown cultures, all of the mutants showed lower fluorescence recovery rates than the wild type (Table 3), consistent with the involvement of these septal proteins in the exchange of esculin among vegetative cells. However, slower residual esculin exchange was observed even in the triple mutant (Table 3), as is also the case with calcein and 5-CF (Table 2). The Δ*sepJ* mutant does not grow diazotrophically and is arrested early in heterocyst differentiation (46) and so cannot be used to test for the involvement of SepJ in esculin exchange between vegetative cells and heterocysts. However, while the Δ*fraC* Δ*fraD* mutant is also incapable of sustained diazotrophic growth, it survives for more than 48 h following a nitrogen step down, producing heterocysts during this time (27). This allows a test for the involvement of FraC and FraD in heterocyst–vegetative-cell exchange. FRAP shows that the transfer of esculin into Δ*fraC* Δ*fraD* heterocysts is slower than in the wild type by a factor of >3 (Table 3).

Loss of metabolic communication in older heterocysts. In wild-type *Anabaena* grown diazotrophically for 48 h, some heterocysts show no esculin fluorescence, despite the presence of esculin in the neighboring vegetative cells (Fig. 6A and B). This suggests that some heterocysts are deficient in esculin exchange with their vegetative neighbors. We quantified esculin equilibration between heterocysts and vegetative cells by dividing the esculin fluorescence intensity in each heterocyst by the mean fluorescence intensity in its immediate vegetative neighbors (I_H/I_V ratio). The I_H/I_V ratio should be ~1 for "communicating" heterocysts, where esculin equilibrates across the cell junctions, but ~0 for heterocysts that are deficient in esculin exchange and also incapable of direct esculin uptake. The I_H/I_V ratio shows a bimodal distribution with peaks close to 0 and 1 (Fig. 6C), consistent with two such populations of heterocysts. Fluorescence in the noncommunicating heterocysts was not significantly above the background seen in unlabeled cells. Communicating and noncommunicating heterocysts are sometimes present in the same *Anabaena* filament (Fig. 6B). The frequency of communicating heterocysts is almost 100% 24 h after a nitrogen step down but then drops to ~70% at 48 h and subsequently remains at that level (Fig. 6D). Therefore, young heterocysts are nearly all capable of esculin exchange, but during continued diazotrophic growth, a population of ~30% of noncommunicating heterocysts builds up. Communicating and noncommunicating heterocysts are equally likely to be located at the terminus of the filament: we found that at 48 h after a nitrogen

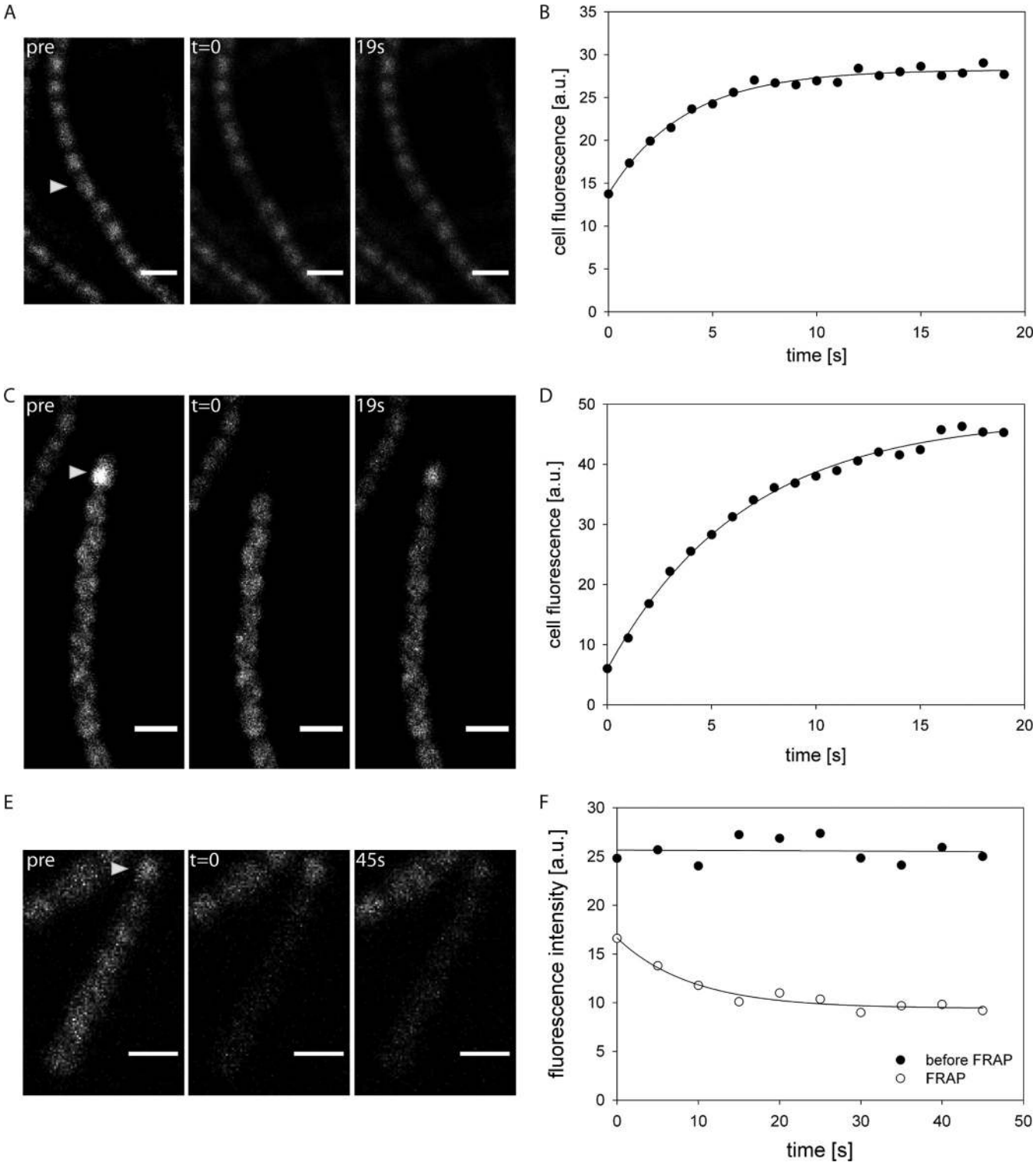

FIG 5 Examples of FRAP experiments monitoring intercellular exchange of esculin in wild-type *Anabaena* filaments. A and B, esculin exchange among vegetative cells; C and D, esculin transfer from vegetative cells to a terminal heterocyst; E and F, esculin transfer from a terminal heterocyst to vegetative cells. (A, C, and E) Fluorescence images from FRAP time series showing esculin fluorescence prior to bleaching (pre), immediately after bleaching ($t = 0$), and at the later time points indicated. Scale bars, 5 μm. (B and D) Fluorescence recovery curves for bleached cells. Fluorescence is expressed in consistent arbitrary units (a.u.). (E and F) Esculin movement from a terminal heterocyst (arrowhead) to the neighboring vegetative cells, observed by monitoring heterocyst fluorescence after bleaching of all of the vegetative cells. Filled circles, heterocyst fluorescence in successive images prior to bleaching. Open circles, heterocyst fluorescence versus time after bleaching fluorescence in the vegetative cells. Heterocyst fluorescence at $t = 0$ is already lowered by diffusion of esculin out of the heterocyst during bleaching, probably combined with some direct bleaching of the heterocyst esculin due to scattered light.

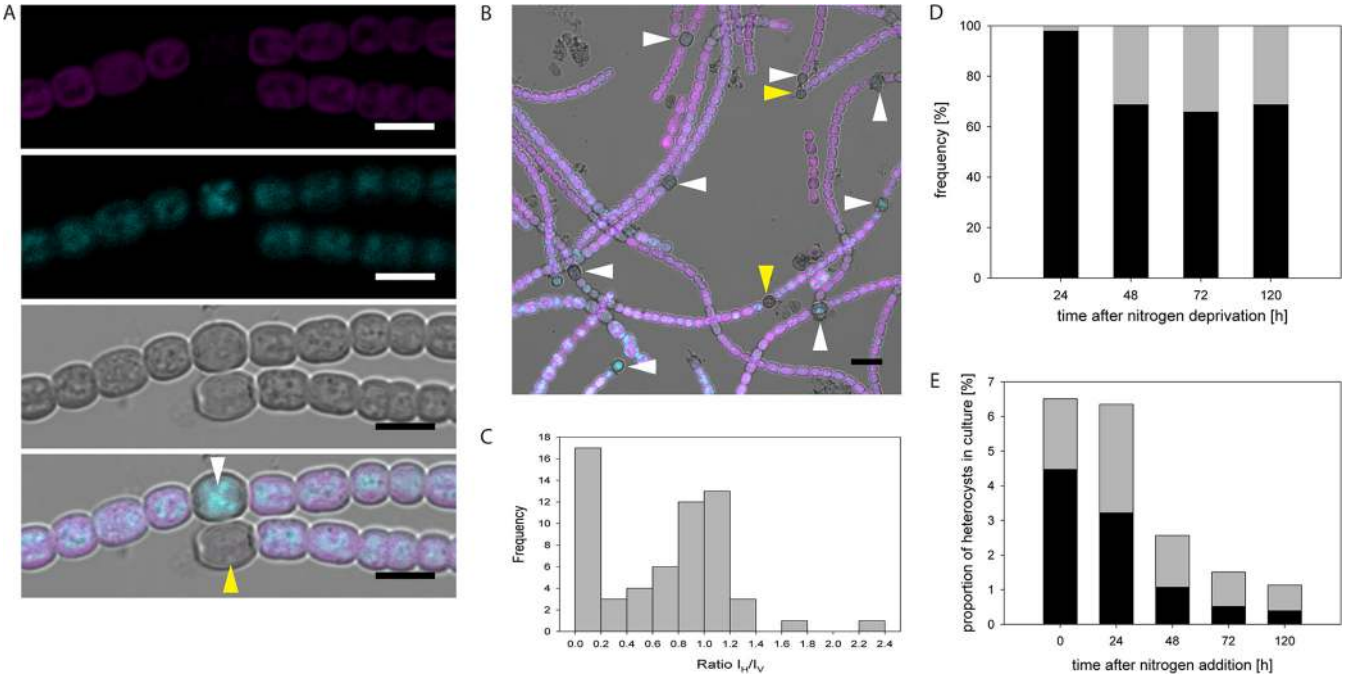

FIG 6 Esculin labeling of *Anabaena* heterocysts. (A and B) Fluorescence micrographs showing esculin-labeled wild-type *Anabaena* filaments 48 h after a combined-nitrogen step down. Communicating heterocysts are indicated by white arrows, and noncommunicating heterocysts (defined by an I_H/I_V ratio of <0.2) are indicated by yellow arrows. I_H, esculin fluorescence intensity in the heterocyst; I_V, mean esculin fluorescence intensity in immediately neighboring vegetative cells. Chlorophyll fluorescence is magenta, esculin fluorescence is cyan, and the bright-field image is in grayscale. Panels A (bottom) and B are merged images. Scale bars, 5 μm in panel A and 10 μm in panel B. (C) Frequency distribution of I_H/I_V ratios for heterocysts in filaments esculin labeled as in panels A and B. (D and E) Frequencies of communicating (black) and noncommunicating (gray) heterocysts versus time following a combined-nitrogen step down (D) and after the addition of combined nitrogen to a diazotrophic culture (E). Detached heterocysts were not included in the statistics.

step down, 52% of noncommunicating heterocysts were terminal ($n = 42$) and also that 52% of communicating heterocysts were terminal ($n = 149$). This suggests that loss of communication is not a consequence of filament breakage. A *cphA1* mutant deficient in cyanophycin synthetase (52) showed a similar frequency of noncommunicating heterocysts (see Fig. S9 in the supplemental material), indicating that cyanophycin plugs are also not the cause of heterocyst noncommunication. Heterocysts are incapable of further cell division and have a limited lifetime before they senesce and die (56). To test the possibility that the noncommunicating heterocysts are senescent, we restored combined nitrogen to a diazotrophic culture. This prevents the generation of new heterocysts, therefore leading to an aging heterocyst population and the gradual disappearance of heterocysts from the culture (57). Heterocyst frequency decreases following combined-nitrogen addition, with a simultaneous decrease in the proportion of communicating heterocysts (Fig. 6E). This suggests that the noncommunicating heterocysts are those in the early stages of senescence, prior to any obvious morphological changes (Fig. 6A).

DISCUSSION

Esculin is a fluorescent tracer that closely resembles sucrose (Table 1). We found that esculin is imported into the cytoplasm of *Anabaena* cells by a sucrose uptake system (Fig. 4), as it is in plants (48). Therefore, imaging of esculin fluorescence in *Anabaena* should give a good guide to the behavior of sucrose. Esculin in the *Anabaena* cytoplasm includes a mobile pool that rapidly and reversibly exchanges among vegetative cells and between vegetative cells and heterocysts (Fig. 5). Esculin fluorescence could not be detected in the periplasm (Fig. 3 and 6; see Fig. S6 in the supplemental material), and exchange is reduced in mutants lacking septal junction proteins, suggesting that the major route for intercellular transfer of esculin is diffusion from cytoplasm to cytoplasm across cell junctions. Communicating heterocysts showed, on average, levels of esculin fluorescence similar to those of their vegetative neighbors (Fig. 6C), suggesting full equilibration of esculin across the cell junction. Reversible heterocyst–vegetative-cell exchange is also indicated by the similar kinetics of esculin movement in both directions (Fig. 5).

Our findings on the ultrastructure and molecular exchange characteristics of a mutant lacking septal proteins shed light on the mechanism of intercellular esculin exchange. Structures that have been termed microplasmodesmata or septosomes have long been known to be present in the intercellular septa of the filaments of heterocyst-forming cyanobacteria (29, 58–60). Cell wall perforations that have been termed nanopores, recently reported to be present in septal peptidoglycan discs (38), may be the places where these structures traverse the murein sacculus (30, 32, 39, 40, 43). Three known proteins that are required for making long filaments in *Anabaena*, SepJ, FraC, and FraD, are located at the intercellular septa where they appear to play a role in cell-cell adhesion and facilitating communication between adjacent cells (23, 24, 26). Such functions would require a physical interaction between the proteins contributed by each of the adjacent cells, implying that these proteins traverse the septal peptidoglycan. We found a significantly decreased number of nanopores in mutants lacking combinations of SepJ, FraC, and FraD compared to the wild type.

The mutants lack the typical nanopore array seen in the wild type and instead show just a few randomly placed nanopores. A straightforward hypothesis is that SepJ, FraC, and FraD are components of the septal junctions and that septal junction complexes containing these proteins influence the activity of the AmiC type amidases to form a septal nanopore array. However, the presence of a few residual nanopores in the Δ*fraC* Δ*fraD* Δ*sepJ* triple mutant indicates either that there are peptidoglycan hydrolases that can form some pores in the absence of any septal junction proteins or that other septal junction proteins, yet to be identified, are present in the intercellular septa. Interestingly, the residual nanopores have a significantly greater mean diameter than those seen in the wild type (see Fig. S5 in the supplemental material). This is consistent with the idea that the residual septal channels in the Δ*sepJ* Δ*fraC* Δ*fraD* triple mutant have a molecular composition different from that of the majority of the channels seen in the wild type, which are likely to include SepJ, FraC, and FraD among their components.

In the Δ*sepJ* Δ*fraC* Δ*fraD* triple mutant, the cytoplasmic membranes of the adjacent cells are very close to each other, and a highly electron-dense layer (presumably peptidoglycan) is observed between them. Intercellular junctions that are thinner than in the wild type have also been observed in the Δ*sepJ* single mutant strain CSVM34 (30). As with metazoan gap junctions (31), septal junction complexes might determine a fixed distance between the cytoplasmic membranes of the adjacent cells, and the absence of those complexes might produce the collapse of the septum between those cells. Mutants lacking SepJ show lower labeling with a fluorescent vancomycin derivative (Fig. 1; see Fig. S3 in the supplemental material), which is indicative of a lower rate of septal peptidoglycan remodeling (38) in the absence of this protein.

Mutants lacking SepJ, FraC, and FraD are all impaired in intercellular esculin exchange (Table 3), consistent with the idea that the septal junctions are crucial for sucrose exchange between cells. Loss of FraC and FraD slows esculin exchange between vegetative cells and heterocysts by about 70% and slows esculin exchange among vegetative cells by about 50% (Table 3). FraC and FraD are involved in the organization of SepJ at the septa (26), which may explain why esculin exchange is as strongly affected in the Δ*fraC* Δ*fraD* mutant strain as in the Δ*sepJ* Δ*fraC* Δ*fraD* triple mutant (Table 3). SepJ, FraC, and FraD (and possibly other proteins) may form a family of intercellular channels with different selectivities for molecular size and charge. Residual intercellular exchange of esculin and fluorescein derivatives in the triple mutant may be due to additional, uncharacterized channels better capable of transmitting esculin than larger and more negatively charged molecules (Table 1). This is consistent with the residual septal nanopores in the triple mutant (Fig. 2).

A route for exchange of carbon and nitrogen compounds between heterocysts and vegetative cells could involve diffusion through a continuous periplasm (22), followed by active import into the cytoplasm (57). However, the rapid exchange of esculin at heterocyst–vegetative-cell septal junctions suggests that diffusion from cytoplasm to cytoplasm across these junctions is the main route for sucrose transfer. Metazoan gap junctions provide a precedent for a protein family (in this case, connexins) forming a range of diffusion channels with different permeability characteristics (31). Some *Anabaena* septal junction structures could be optimized for the exchange of sucrose, consistent with the idea that sucrose is the principal metabolite used to supply heterocysts with photosynthate (12–15).

During prolonged diazotrophic growth, ~30% of heterocysts do not show esculin fluorescence (Fig. 6). Although heterocysts might be capable of direct sucrose uptake (57), the noncommunicating heterocysts must be incapable of esculin uptake by this route, and from the neighboring vegetative cells, since their esculin fluorescence is negligible (Fig. 6). Changes in the noncommunicating population following removal and readdition of combined nitrogen (Fig. 6) suggest that this population consists of heterocysts in the early stages of senescence. Heterocysts can consume ~50% of the filament's photosynthate (1), so it must be important to supply only fully functional heterocysts with sucrose. It may be crucial for survival to close communication with a dying heterocyst before it lyses, to avoid rapid leakage of metabolites into the medium. Loss of communication could result from closure of half-channels on either side of the heterocyst–vegetative-cell septal junction, perhaps comparable to the regulation of metazoan gap junction activity (61). The partitioning of sucrose between communicating cells in the filament may be controlled by sucrose metabolism in individual cells, a simple but effective way to ensure that the photosynthate supply meets the photosynthate demand of individual vegetative cells and heterocysts.

MATERIALS AND METHODS

Strains, growth conditions, and PCR analysis. The *sepJ*, *fraC*, and *fraD* genes are open reading frames *alr2338*, *alr2392*, and *alr2393* of the *Anabaena* genome, respectively (62). Mutant strains CSS7 (*cphA1*::C.S3), CSVT22 (Δ*fraC* Δ*fraD*), and CSVM34 (Δ*sepJ*) have been previously described (27, 46, 55). Strain CSVM141 was constructed by transferring an inactivating *sepJ* construct to mutant CSVT22 as previously described for the construction of CSVM34 from strain PCC 7120 (46). CSVM141 carries unmarked deletions in *fraC*, *fraD*, and *sepJ*. DNA was isolated from *Anabaena* as described in reference 63. PCR was performed by standard procedures (64), and the PCR products were resolved by electrophoresis in 0.8% agarose gels. For the oligodeoxynucleotide primers used, see Table S1 in the supplemental material.

Anabaena strains were grown in liquid BG11 medium (65) with antibiotics appropriate for mutant strain CSS7 in conical flasks with shaking (80 to 100 rpm) at 30°C in white light at ~15 to 75 $\mu E \cdot m^{-2} \cdot s^{-1}$. Heterocyst formation was induced by growth in $BG11_0$ medium (65), which lacks combined nitrogen. For transfer between media, cells were harvested by centrifugation (3,000 × *g*) and washed three times in the appropriate medium. To determine filament length, flasks containing BG11 medium were inoculated with material from plates and incubated for 3 to 4 days at 30°C (80 to 90 rpm, 25 $\mu E \cdot m^{-2} \cdot s^{-1}$). The cultures were then harvested, adjusted to 2 μg of chlorophyll *a* (Chl) $\cdot$ ml^{-1} and incubated in fresh BG11 medium for 24 h. Filaments were counted at that time or harvested, washed, and resuspended in $BG11_0$ medium and further incubated under the culture conditions described above. Samples were taken with great care to prevent disruption of the filaments and placed on solidified medium (BG11 or $BG11_0$). Samples were visualized and photographed by standard light microscopy.

Electron microscopy. Ultrathin section preparation was done as described in reference 40. Briefly, filaments of the strains indicated that were grown in BG11 medium were harvested by gentle centrifugation and fixed with 4% (wt/vol) glutaraldehyde and 2% (wt/vol) $KMnO_4$, dehydrated with increasing concentrations of ethanol, and embedded in araldite, and ultrathin sections were prepared and poststained with uranyl acetate and lead citrate (66). The samples were examined with a JEOL JEM-1230 electron microscope at 80 kV. The sacculi were isolated and analyzed as previously described (38, 67). In brief, after breakage of the cells by soni-

cation and subsequent homogenization with glass beads, the broken filaments were added dropwise to boiling SDS and boiled for several hours. After ultracentrifugation (Beckmann 75 Ti rotor, 322,000 × *g*, 25°C, 45 min), the pellet was dissolved in H_2O and boiled again with SDS. After the procedure was repeated, the sacculi were treated with chymotrypsin and again boiled in SDS. After being washed with H_2O, the purified sacculi were put on Formvar/carbon film-coated copper grids, stained with uranyl acetate, and visualized with a Philips Tecnai-10 microscope at 80 kV (37, 67).

Van-FL staining. Vanc-FL staining of BG11-grown filaments of the strains indicated was performed as previously reported (38). Samples were visualized in a Leica DM6000B fluorescence microscope with an ORCA-ER camera (Hamamatsu). Fluorescence was monitored with a fluorescein isothiocyanate L5 filter (excitation, 480/40-nm band-pass [BP] filter; emission, 527/30-nm BP filter). Images were treated with the Leica Application Suite Advanced Fluorescence software and merged with ImageJ 1.47i software (http://imagej.nih.gov/ij).

Labeling, fluorescence microscopy, and FRAP with esculin. Filaments were harvested, resuspended in 500 μl of fresh growth medium, mixed with 15 μl of saturated (~5 mM) aqueous esculin hydrate solution (Sigma-Aldrich), and incubated for 30 min in the dark with gentle shaking at 30°C prior to being washed three times in growth medium, followed by incubation in the dark for 15 min in 1 ml of medium at 30°C with gentle shaking. Cells were then washed again and spotted onto a BG11 or $BG11_0$ agar plate (1% [wt/vol]), and excess medium was removed. Heterocyst counts (Fig. 6; see Fig. S9 in the supplemental material) used alcian blue staining to highlight the heterocysts (68); this did not perturb fluorescence imaging. Five microliters of 0.5% (wt/vol) alcian blue 8GX solution in 50% (vol/vol) ethanol (Acros Organics) was added to the esculin-labeled cell suspension (68). Samples were prepared as described above but without the final washing step. Small blocks of agar with cells adsorbed onto the surface were placed in a custom-built, temperature-controlled sample holder under a glass coverslip at 30°C. Cells were visualized with a confocal laser scanning microscope (Leica TCS SP5) with a 63× oil immersion objective (numerical aperture [NA] 1.4). Fluorescence was excited at 355 nm, and esculin was detected at 443 to 490 nm and Chl was detected at 670 to 720 nm. High-resolution imaging used 6× line-average with an optical section of ~0.7 μm. FRAP measurements were made without line averaging and with a wider pinhole giving an optical section of ~4 μm. After capturing a prebleaching image, the fluorescence of the defined region of interest (ROI) was bleached out by scanning the ROI at an ~6× higher laser intensity, and recovery was then recorded in a sequence of full-frame images. To investigate the efficiency of heterocyst labeling, we used additional excitation at 488 nm for better bright-field imaging. Images were processed with ImageJ software (69).

Labeling, fluorescence microscopy, and FRAP with calcein and 5-CF. For calcein and 5-CF transfer assays, calcein and 5-CF staining and FRAP analysis were performed as previously reported. Calcein and 5-CF were loaded into cells as esterified precursors (calcein acetoxymethylester and 5-CF diacetate acetoxymethylester) (23, 27). Cell suspensions were spotted onto agar and placed in a custom-built temperature-controlled sample holder with a glass coverslip on top. All measurements were carried out at 30°C. For both calcein and 5-CF, cells were imaged with a Leica HCX Plan Apo 63× NA 1.4 oil immersion objective attached to a Leica TCS SP5 confocal laser scanning microscope as previously described for calcein (23) with a 488-nm line argon laser as the excitation source. Fluorescence emission was monitored by collection across windows of 500 to 520 or 500 to 527 nm in different experiments with a 150-μm pinhole. After an initial image was recorded, bleaching was carried out by an automated FRAP routine that switched the microscope to X-scanning mode, increased the laser intensity by a factor of 10, and scanned a line across one cell for 0.137 s before reducing the laser intensity, switching back to XY imaging mode, and recording a sequence of images typically at 1-s intervals.

FRAP data analysis. The "exchange coefficient" E relates the rate of dye movement between two adjacent cells to the difference in dye concentration between the cells (23). However, the high immobile fraction (F_i) for esculin and 5-CF (27) (Table 3) prevented the quantitation of E for exchange among vegetative cells, which requires fitting of the simulated time development of dye distribution in the filament to the experimental data (23). We therefore used a simpler way to quantify kinetics of esculin transfer between vegetative cells by measuring the recovery rate constant R from the formula $C_B = C_0 + C_R(1 - e^{-2Rt})$, where C_B is fluorescence in the bleached cell, C_0 is fluorescence immediately after bleaching and tending toward $C_0 + C_R$ after fluorescence recovery, R is the recovery rate constant, and t is time (27). For valid comparison of terminal cells (with one cell junction) with cells in the middle of filaments (with two cell junctions), the formula $C_B = C_0 + C_R(1 - e^{-Rt})$ was used in the former case.

Esculin uptake and sucrose competition. *Anabaena* cultures grown in BG11 medium were, when indicated, harvested by centrifugation, washed with $BG11_0$ medium, and incubated for 18 h in $BG11_0$ medium under culture conditions. Cells were harvested, washed, and resuspended in growth medium supplemented with 10 mM HEPES-NaOH buffer (pH 7) with or without 10 mM sucrose. Esculin was added to 100 μM, and suspensions were incubated at 30°C in the light (~170 $\mu E \cdot m^{-2} \cdot s^{-1}$). One-milliliter samples were withdrawn and filtered. Cells on the filters were washed and resuspended in 2 ml of 10 mM HEPES-NaOH buffer (pH 7). Fluorescence was measured in a Varian Cary Eclipse Fluorescence Spectrophotometer (excitation wavelength, 360 ± 10 nm; emission wavelength, 462 ± 10 nm). Esculin solutions in the same buffer were used as standards.

Physicochemical properties of dyes. Tools at http://www.chemicalize.org/ and Marvin 6.0.2 (ChemAxon) were used to predict molecular properties.

SUPPLEMENTAL MATERIAL

Supplemental material for this article may be found at http://mbio.asm.org/lookup/suppl/doi:10.1128/mBio.02109-14/-/DCSupplemental.

Figure S1, TIF file, 0.1 MB.
Figure S2, TIF file, 0.1 MB.
Figure S3, TIF file, 0.05 MB.
Figure S4, TIF file, 2.1 MB.
Figure S5, TIF file, 0.04 MB.
Figure S6, TIF file, 0.6 MB.
Figure S7, TIF file, 1 MB.
Figure S8, TIF file, 0.5 MB.
Figure S9, TIF file, 1.1 MB.
Table S1, DOC file, 0.03 MB.

ACKNOWLEDGMENTS

D.J.N. was supported by a Queen Mary University of London College studentship. M.N.M. was the recipient of an FPU (Formación del Personal Universitario) fellowship from the Spanish Government. Work in Seville was supported by grant BFU2011-22762 from Plan Nacional de Investigación, Spain, cofinanced by the European Regional Development Fund, and by Plan Andaluz de Investigación, Regional Government of Andalucía (grant P10-CVI-6665). Research in Tübingen was supported by the Deutsche Forschungsgemeinschaft (SFB766).

We thank Thomas Volkmer and Wolfgang Lockau (Humboldt Universität zu Berlin) for providing cyanophycin, and we thank Karl Forchhammer (University of Tübingen) for helpful discussion and support.

REFERENCES

1. **Wolk CP.** 1996. Heterocyst formation. Annu Rev Genet **30**:59–78. http://dx.doi.org/10.1146/annurev.genet.30.1.59.
2. **Kumar K, Mella-Herrera RA, Golden JW.** 2010. Cyanobacterial heterocysts. Cold Spring Harb Perspect Biol **2**:a000315. http://dx.doi.org/10.1101/cshperspect.a000315.

3. **Wilcox M, Mitchison GJ, Smith RJ.** 1973. Pattern formation in the blue-green alga, *Anabaena*. I. Basic mechanisms. J Cell Sci **12:**707–723.
4. **Yoon H.-S, Golden JW.** 1998. Heterocyst pattern formation controlled by a diffusible peptide. Science **282:**935–938. http://dx.doi.org/10.1126/science.282.5390.935.
5. **Huang X, Dong Y, Zhao J.** 2004. HetR homodimer is a DNA-binding protein required for heterocyst differentiation, and the DNA-binding activity is inhibited by PatS. Proc Natl Acad Sci U S A **101:**4848–4853. http://dx.doi.org/10.1073/pnas.0400429101.
6. **Corrales-Guerrero L, Mariscal V, Flores E, Herrero A.** 2013. Functional dissection and evidence for intercellular transfer of the heterocyst-differentiation PatS morphogen. Mol Microbiol **88:**1093–1105. http://dx.doi.org/10.1111/mmi.12244.
7. **Walsby AE.** 2007. Cyanobacterial heterocysts: terminal pores proposed as sites of gas exchange. Trends Microbiol **15:**340–349. http://dx.doi.org/10.1016/j.tim.2007.06.007.
8. **Thomas J, Meeks JC, Wolk CP, Shaffer PW, Austin SM.** 1977. Formation of glutamine from [13n]ammonia, [13n]dinitrogen, and [14C]glutamate by heterocysts isolated from *Anabaena cylindrica*. J Bacteriol **129:**1545–1555.
9. **Martín-Figueroa E, Navarro F, Florencio FJ.** 2000. The GS-GOGAT pathway is not operative in the heterocysts. Cloning and expression of *glsF* gene from the cyanobacterium *Anabaena* sp. PCC7120. FEBS Lett **476:**282–286. http://dx.doi.org/10.1016/S0014-5793(00)01722-1.
10. **Richter R, Hejazi M, Kraft R, Ziegler K, Lockau W.** 1999. Cyanophycinase, a peptidase degrading the cyanobacterial reserve material multi-L-arginyl-poly-L-aspartic acid (cyanophycin): molecular cloning of the gene of *Synechocystis* sp. PCC 6803, expression in *Escherichia coli*, and biochemical characterization of the purified enzyme. Eur J Biochem **263:**163–169. http://dx.doi.org/10.1046/j.1432-1327.1999.00479.x.
11. **Burnat M, Herrero A, Flores E.** 2014. Compartmentalized cyanophycin metabolism in the diazotrophic filaments of a heterocyst-forming cyanobacterium. Proc Natl Acad Sci U S A **111:**3823–3828. http://dx.doi.org/10.1073/pnas.1318564111.
12. **Schilling N, Ehrnsperger K.** 1985. Cellular differentiation of sucrose metabolism in *Anabaena variabilis*. Z Naturforsch **70:**776–779.
13. **Curatti L, Flores E, Salerno G.** 2002. Sucrose is involved in the diazotrophic metabolism of the heterocyst-forming cyanobacterium *Anabaena* sp. FEBS Lett **513:**175–178. http://dx.doi.org/10.1016/S0014-5793(02)02283-4.
14. **López-Igual R, Flores E, Herrero A.** 2010. Inactivation of a heterocyst-specific invertase indicates a principal role of sucrose catabolism in heterocysts of *Anabaena* sp. J Bacteriol **192:**5526–5533. http://dx.doi.org/10.1128/JB.00776-10.
15. **Vargas WA, Nishi CN, Giarrocco LE, Salerno GL.** 2011. Differential roles of alkaline/neutral invertases in *Nostoc* sp. PCC 7120: Inv-B isoform is essential for diazotrophic growth. Planta **233:**153–162. http://dx.doi.org/10.1007/s00425-010-1288-5.
16. **Jüttner F.** 1983. ^{14}C-labelled metabolites in heterocysts and vegetative cells of *Anabaena cylindrica* filaments and their presumptive function as transport vehicles of organic carbon and nitrogen. J Bacteriol 155:628–633.
17. **Pernil R, Herrero A, Flores E.** 2010. Catabolic function of compartmentalized alanine dehydrogenase in the heterocyst-forming cyanobacterium *Anabaena* sp. strain PCC 7120. J Bacteriol **192:**5165–5172. http://dx.doi.org/10.1128/JB.00603-10.
18. **Haselkorn R.** 2008. Cell-cell communication in filamentous cyanobacteria. Mol Microbiol **70:**783–785. http://dx.doi.org/10.1111/j.1365-2958.2008.06475.x.
19. **Mariscal V, Flores E.** 2010. Multicellularity in a heterocyst-forming cyanobacterium: pathways for intercellular communication. Adv Exp Med Biol **675:**123–135. http://dx.doi.org/10.1007/978-1-4419-1528-3_8.
20. **Flores E, Herrero A.** 2010. Compartmentalized function through cell differentiation in filamentous cyanobacteria. Nat Rev Microbiol **8:**39–50. http://dx.doi.org/10.1038/nrmicro2242.
21. **Flores E, Herrero A, Wolk CP, Maldener I.** 2006. Is the periplasm continuous in filamentous cyanobacteria? Trends Microbiol **14:**439–443. http://dx.doi.org/10.1016/j.tim.2006.08.007.
22. **Mariscal V, Herrero A, Flores E.** 2007. Continuous periplasm in a filamentous, heterocyst-forming cyanobacterium. Mol Microbiol **65:**1139–1145. http://dx.doi.org/10.1111/j.1365-2958.2007.05856.x.
23. **Mullineaux CW, Mariscal V, Nenninger A, Khanum H, Herrero A, Flores E, Adams DG.** 2008. Mechanism of intercellular molecular exchange in heterocyst-forming cyanobacteria. EMBO J **27:**1299–1308. http://dx.doi.org/10.1038/emboj.2008.66.
24. **Flores E, Pernil R, Muro-Pastor AM, Mariscal V, Maldener I, Lechno-Yossef S, Fan Q, Wolk CP, Herrero A.** 2007. Septum-localized protein required for filament integrity and diazotrophy in the heterocyst-forming cyanobacterium *Anabaena* sp. strain PCC 7120. J Bacteriol **189:**3884–3890. http://dx.doi.org/10.1128/JB.00085-07.
25. **Nayar AS, Yamaura H, Rajagopalan R, Risser DD, Callahan SM.** 2007. FraG is necessary for filament integrity and heterocyst maturation in the cyanobacterium *Anabaena* sp. strain PCC 7120. Microbiology **153:**601–607. http://dx.doi.org/10.1099/mic.0.2006/002535-0.
26. **Merino-Puerto V, Mariscal V, Mullineaux CW, Herrero A, Flores E.** 2010. Fra proteins influencing filament integrity, diazotrophy and localization of septal protein SepJ in the heterocyst-forming cyanobacterium *Anabaena* sp. Mol Microbiol **75:**1159–1170. http://dx.doi.org/10.1111/j.1365-2958.2009.07031.x.
27. **Merino-Puerto V, Schwarz H, Maldener I, Mariscal V, Mullineaux CW, Herrero A, Flores E.** 2011. FraC/FraD-dependent intercellular molecular exchange in the filaments of a heterocyst-forming cyanobacterium, *Anabaena* sp. Mol Microbiol **82:**87–98. http://dx.doi.org/10.1111/j.1365-2958.2011.07797.x.
28. **Giddings THJ, Staehelin LA.** 1978. Plasma membrane architecture of *Anabaena cylindrica*: occurrence of microplasmodesmata and changes associated with heterocyst development and the cell cycle. Cytobiologie **16:**235–249.
29. **Giddings TH, Staehelin LA.** 1981. Observation of microplasmodesmata in both heterocyst-forming and non-heterocyst forming filamentous cyanobacteria by freeze-fracture electron microscopy. Arch Microbiol **129:**295–298. http://dx.doi.org/10.1007/BF00414700.
30. **Wilk L, Strauss M, Rudolf M, Nicolaisen K, Flores E, Kühlbrandt W, Schleiff E.** 2011. Outer membrane continuity and septosome formation between vegetative cells in the filaments of *Anabaena* sp. PCC 7120. Cell Microbiol **13:**1744–1754. http://dx.doi.org/10.1111/j.1462-5822.2011.01655.x.
31. **Koval M.** 2006. Pathways and control of connexin oligomerization. Trends Cell Biol **16:**159–166. http://dx.doi.org/10.1016/j.tcb.2006.01.006.
32. **Mariscal V.** 2014. Cell-cell joining proteins in heterocyst-forming cyanobacteria, p 293159–304. In Flores E, Herrero A (ed), The cell biology of Cyanobacteria. Caister Academic Press, Norfolk, England.
33. **Drews G.** 1973. Fine structure and chemical composition of the cell envelopes, p 99159–116. In Carr NG, Whitton BA (ed), The biology of blue-green algae. University of California Press, Berkeley, CA.
34. **Hoiczyk E, Hansel A.** 2000. Cyanobacterial cell walls: news from an unusual prokaryotic envelope. J Bacteriol **182:**1191–1199. http://dx.doi.org/10.1128/JB.182.5.1191-1199.2000.
35. **Vollmer W, Seligman SJ.** 2010. Architecture of peptidoglycan: more data and more models. Trends Microbiol **18:**59–66. http://dx.doi.org/10.1016/j.tim.2009.12.004.
36. **Dunn JH, Wolk CP.** 1970. Composition of the cellular envelopes of *Anabaena cylindrica*. J Bacteriol **103:**153–158.
37. **Lehner J, Zhang Y, Berendt S, Rasse TM, Forchhammer K, Maldener I.** 2011. The morphogene AmiC2 is pivotal for multicellular development in the cyanobacterium *Nostoc punctiforme*. Mol Microbiol **79:**1655–1669. http://dx.doi.org/10.1111/j.1365-2958.2011.07554.x.
38. **Lehner J, Berendt S, Dörsam B, Pérez R, Forchhammer K, Maldener I.** 2013. Prokaryotic multicellularity: a nanopore array for bacterial cell communication. FASEB J **27:**2293–2300. http://dx.doi.org/10.1096/fj.12-225854.
39. **Palinska KA, Krumbein WE.** 2000. Perforation patterns in the peptidoglycan wall of filamentous cyanobacteria. J Phycol **36:**139–145. http://dx.doi.org/10.1046/j.1529-8817.2000.99040.x.
40. **Nürnberg DJ, Mariscal V, Parker J, Mastroianni G, Flores E, Mullineaux CW.** 2014. Branching and intercellular communication in the section V cyanobacterium *Mastigocladus laminosus*, a complex multicellular prokaryote. Mol Microbiol **91:**935–949. http://dx.doi.org/10.1111/mmi.12506.
41. **Omairi-Nasser A, Haselkorn R, Austin J, II.** 2014. Visualization of channels connecting cells in filamentous nitrogen-fixing cyanobacteria. FASEB J **28:**3016–3022. http://dx.doi.org/10.1096/fj.14-252007.
42. **Berendt S, Lehner J, Zhang YV, Rasse TM, Forchhammer K, Maldener I.** 2012. Cell wall amidase AmiC1 is required for cellular communication and heterocyst development in the cyanobacterium *Anabaena* PCC 7120

but not for filament integrity. J Bacteriol **194:**-5218–5227. http://dx.doi.org/10.1128/JB.00912-12.
43. **Maldener I, Summers ML, Sukenik A.** 2014. Cellular differentiation in filamentous cyanobacteria, p 2635218–292. In Flores E, Herrero A (ed), The cell biology of Cyanobacteria. Caister Academic Press, Norfolk, England.
44. **Zhang L.-C, Chen Y.-F, Chen W.-L, Zhang C.-C.** 2008. Existence of periplasmic barriers preventing green fluorescent protein diffusion from cell to cell in the cyanobacterium *Anabaena* sp. strain PCC 7120. Mol Microbiol **70:**814–823. http://dx.doi.org/10.1111/j.1365-2958.2008.06476.x.
45. **Zhang L.-C, Risoul V, Latifi A, Christie JM, Zhang C.-C.** 2013. Exploring the size-limit of protein diffusion through the periplasm in cyanobacterium *Anabaena* sp. PCC7120 using the 13 kDa iLOV fluorescent protein. Res Microbiol **164:**710–717. http://dx.doi.org/10.1016/j.resmic.2013.05.004.
46. **Mariscal V, Herrero A, Nenninger A, Mullineaux CW, Flores E.** 2011. Functional dissection of the three-domain SepJ protein joining the cells in cyanobacterial trichomes. Mol Microbiol **79:**1077–1088. http://dx.doi.org/10.1111/j.1365-2958.2010.07508.x.
47. **Reinders A, Sivitz AB, Ward JM.** 2012. Evolution of plant sucrose uptake transporters. Front Plant Sci **3:**22. http://dx.doi.org/10.3389/fpls.2012.00022.
48. **Gora PJ, Reinders A, Ward JM.** 2012. A novel fluorescent assay for sucrose transporters. Plant Methods **8:**13. http://dx.doi.org/10.1186/1746-4811-8-13.
49. **Reinders A, Sun Y, Karvonen KL, Ward JM.** 2012. Identification of amino acids important for substrate specificity in sucrose transporters using gene shuffling. J Biol Chem **287:**30296–30304. http://dx.doi.org/10.1074/jbc.M112.372888.
50. **Sivitz AB, Reinders A, Johnson ME, Krentz AD, Grof CP, Perroux JM, Ward JM.** 2007. *Arabidopsis* sucrose transporter AtSUC9. High-affinity transport activity, intragenic control of expression, and early flowering mutant phenotype. Plant Physiol **143:**188–198. http://dx.doi.org/10.1104/pp.106.089003.
51. **Yin Z, Hüve K, Heber U.** 1996. Light-dependent proton transport into mesophyll vacuoles of leaves of C_3 plants as revealed by pH-indicating fluorescent dyes: a reappraisal. Planta **199:**9–17. http://dx.doi.org/10.1007/BF00196875.
52. **Blanco-Rivero A, Leganés F, Fernández-Valiente E, Calle P, Fernández-Piñas F.** 2005. *mrpA*, a gene with roles to resistance to Na^+ and adaptation to alkaline pH in the cyanobacterium *Anabaena* sp. PCC7120. Microbiology **151:**1671–1682. http://dx.doi.org/10.1099/mic.0.27848-0.
53. **Nicolaisen K, Mariscal V, Bredemeier R, Pernil R, Moslavac S, López-Igual R, Maldener I, Herrero A, Schleiff E, Flores E.** 2009. The outer membrane is a permeability barrier for intercellularly exchanged metabolites in a heterocyst-forming cyanobacterium. Mol Microbiol **74:**58–70. http://dx.doi.org/10.1111/j.1365-2958.2009.06850.x.
54. **Zhang Y, Li J, Dong L, Li Y, Chen X.** 2008. Characterization of interaction between esculin and human serum albumin in membrane mimetic environments. J Mol Struct **889:**119–128. http://dx.doi.org/10.1016/j.molstruc.2008.01.040.
55. **Picossi S, Valladares A, Flores E, Herrero A.** 2004. Nitrogen-regulated genes for the metabolism of cyanophycin, a bacterial nitrogen reserve polymer: expression and mutational analysis of two cyanophycin synthetase and cyanophycinase gene clusters in heterocyst-forming cyanobacterium *Anabaena* sp. PCC 7120. J Biol Chem **279:**11582–11592. http://dx.doi.org/10.1074/jbc.M311518200.
56. **Meeks JC, Campbell EL, Summers ML, Wong FC.** 2002. Cellular differentiation in the cyanobacterium *Nostoc punctiforme*. Arch Microbiol **178:**395–403. http://dx.doi.org/10.1007/s00203-002-0476-5.
57. **Park J.-J, Lechno-Yossef S, Wolk CP, Vieille C.** 2013. Cell-specific gene expression in *Anabaena variabilis* grown phototrophically, mixotrophically and heterotrophically. BMC Genomics **14:**759. http://dx.doi.org/10.1186/1471-2164-14-759.
58. **Metzner I.** 1955. Zur Chemie und zum submikroskopischen Aufbau der Zellwände, Scheiden und Gallerten von Cyanophyceen. Arch-Mikrobiologie **22:**45–77. http://dx.doi.org/10.1007/BF00408507.
59. **Wildon DC, Mercer FV.** 1963. The ultrastructure of the heterocyst and akinete of blue-green algae. Archiv Mikrobiol **47:**19–31. http://dx.doi.org/10.1007/BF00408286.
60. **Lang NJ, Fay P.** 1971. The heterocysts of blue-green algae. II. Details of ultrastructure. Proc R Soc Lond B Biol Sci **178:**193–203. http://dx.doi.org/10.1098/rspb.1971.0061.
61. **Oshima A, Tani K, Hiroaki Y, Fujiyoshi Y, Sosinsky GE.** 2007. Three-dimensional structure of a human connexin26 gap junction channel reveals a plug in the vestibule. Proc Natl Acad Sci U S A **104:**10034–10039. http://dx.doi.org/10.1073/pnas.0703704104.
62. **Kaneko T, Nakamura Y, Wolk CP, Kuritz T, Sasamoto S, Watanabe A, Iriguchi M, Ishikawa A, Kawashima K, Kimura T, Kishida Y, Kohara M, Matsumoto M, Matsuno A, Muraki A, Nakazaki N, Shimpo S, Sugimoto M, Takazawa M, Yamada M, Yasuda M, Tabata S.** 2001. Complete genomic sequence of the filamentous nitrogen-fixing cyanobacterium *Anabaena* sp. PCC7120. DNA Res **8:**205–213. http://dx.doi.org/10.1093/dnares/8.5.205.
63. **Cai YP, Wolk CP.** 1990. Use of a conditionally lethal gene in *Anabaena* sp. strain PCC 7120 to select for double recombinants and to entrap insertion sequences. J Bacteriol **172:**3138–3145.
64. **Ausubel FM, Brent R, Kingston RE, Moore DD, Seidman JG, Smith JA, Struhl K.** 2008. Current protocols in molecular biology. Greene Publishing and Wiley Interscience, New York, NY.
65. **Castenholz RW.** 1988. Culturing methods for cyanobacteria. Methods Enzymol **167:**68–93.
66. **Reynolds ES.** 1963. The use of lead citrate at high pH as an electron-opaque stain in electron microscopy. J Cell Biol **17:**208–212. http://dx.doi.org/10.1083/jcb.17.1.208.
67. **de Pedro MA, Quintela JC, Höltje JV, Schwarz H.** 1997. Murein segregation in *Escherichia coli*. J Bacteriol **179:**2823–2834.
68. **Borthakur PB, Orozco CC, Young-Robbins SS, Haselkorn R, Callahan SM.** 2005. Inactivation of patS and hetN causes lethal levels of heterocyst differentiation in the filamentous cyanobacterium *Anabaena* sp. PCC 7120. Mol Microbiol **57:**111–123. http://dx.doi.org/10.1111/j.1365-2958.2005.04678.x.
69. **Abràmoff MD, Magalhães PJ, Ram SJ.** 2004. Image processing with ImageJ. Biophotonics Int **11:**36–42. http://www.imagescience.org/meijering/publications/download/bio2004.pdf.
70. **Berg H, Ziegler K, Piotukh K, Baier K, Lockau W, Volkmer-Engert R.** 2000. Biosynthesis of the cyanobacterial reserve polymer multi-L-arginyl-poly-L-aspartic acid (cyanophycin): mechanism of the cyanophycin synthetase reaction studied with synthetic primers. Eur J Biochem **267:**5561–5570. http://dx.doi.org/10.1146/j.1432-1327.2000.01622.x.